Journal of Power Sources 196 (2011) 10176–10182

Contents lists available at ScienceDirect

Journal of Power Sources

journal homepage: www.elsevier.com/locate/jpowsour

Solvothermal synthesis of hierarchical $LiFePO_4$ microflowers as cathode materials for lithium ion batteries

Qiang Wang[a,b], Weixin Zhang[a,b,*], Zeheng Yang[a,b], Shaoying Weng[a,b], Zhuojie Jin[a,b]

[a] School of Chemical Engineering, Hefei University of Technology, Hefei, Anhui 230009, PR China
[b] Anhui Key Laboratory of Controllable Chemical Reaction & Material Chemical Engineering, Hefei, Anhui 230009, PR China

ARTICLE INFO

Article history:
Received 17 May 2011
Received in revised form 3 August 2011
Accepted 9 August 2011
Available online 16 August 2011

Keywords:
Lithium ion batteries
Lithium iron phosphate
Hierarchical microflower
Solvothermal synthesis
Electrochemical performance

ABSTRACT

Hierarchical $LiFePO_4$ microflowers have been successfully synthesized via a solvothermal reaction in ethanol solvent with the self-prepared ammonium iron phosphate rectangular nanoplates as a precursor, which is obtained by a simple water evaporation method beforehand. The hierarchical $LiFePO_4$ microflowers are self-assemblies of a number of stacked rectangular nanoplates with length of 6–8 μm, width of 1–2 μm and thickness of around 50 nm. When ethanol is replaced with the water–ethanol mixed solvent in the solvothermal reaction, $LiFePO_4$ micro-octahedrons instead of hierarchical microflowers can be prepared. Then both of them are respectively modified with carbon coating through a post-heat treatment and their morphologies are retained. As a cathode material for rechargeable lithium ion batteries, the carbon-coated hierarchical $LiFePO_4$ microflowers deliver high initial discharge capacity (162 mAh g^{-1} at 0.1 C), excellent high-rate discharge capability (101 mAh g^{-1} at 10 C), and cycling stability, which exhibits better electrochemical performances than carbon-coated $LiFePO_4$ micro-octahedrons. These enhanced electrochemical properties can be attributed to the hierarchical micro/nanostructures, which can take advantage of structure stability of micromaterials for long-term cycling. Furthermore the rectangular nanoplates as the building blocks can improve the electrochemical reaction kinetics and finally promote the rate performance.

1. Introduction

Rechargeable lithium-ion batteries are the most promising candidates for applications in electric vehicles (EVs), hybrid electric vehicles (HEVs), and power tools in terms of energy densities and power densities [1–3]. The olivine $LiFePO_4$ is an attractive electrode material for its remarkable advantages, such as low toxicity, low cost, long cycle life and high safety [4]. However, $LiFePO_4$ suffers from poor high-rate capacity due to the low electronic conductivity and slow diffusion of lithium ions, which impede realizing high rate capability, a critical performance for high power applications [4,5].

Tremendous efforts have been made to overcome the inherent limitations of $LiFePO_4$. In addition to doping with metallic elements [6–8] and coating the particles with carbonaceous conductors [9,10] to improve the electronic conductivity, reducing particles to nanometer scale has attracted much attention recently [11], which could shorten the lithium ion transport distances and enhance ionic diffusion rate. For instances, $LiFePO_4$ nanorod [12,13], nanowire [14,15] and nanoplate [16,17] electrode materials have been prepared to improve their capacities and rate performance for lithium ion batteries.

However some nano-sized $LiFePO_4$ cathode materials have low crystallization degree and are difficult to avoid the degradation of discharge capacity on long-time cycling especially at high discharge rate [18,19]. Moreover, the high surface area of nanoparticles also raises the risk of secondary reactions involving electrolyte decomposition between electrode and electrolyte, which causes a high level of irreversibility and poor cycle life to some extent [18]. Furthermore, the low packing density of nanoparticles also limits the total volumetric energy density of lithium-ion batteries [18,20,21].

In recent years, the organization of nanoscale building blocks (nanoparticles, nanorods or nanoribbons) into hierarchical architectures via self-assembly open up new opportunities for development of materials with designed novel properties because they can take the advantages of both nanometer-sized building blocks and micro- or submicrometer-sized assemblies. While the former could provide negligible diffusion time and possible new Li storage mechanism for the favorable kinetics and high capacities, the latter could be beneficial to afford good stability for the electrode materials, which are important for enhancing the cycle performance of electrodes [20,21]. Recently, Cao et al. [22]

* Corresponding author at: School of Chemical Engineering, Hefei University of Technology, Hefei, Anhui 230009, PR China. Tel.: +86 551 2901450; fax: +86 551 2901450.
E-mail address: wxzhang@hfut.edu.cn (W. Zhang).

0378-7753/$ – see front matter © 2011 Elsevier B.V. All rights reserved.
doi:10.1016/j.jpowsour.2011.08.046

reported that hierarchically dumbbell-like $LiFePO_4$ microstructures assembled with tabular particles were prepared by a solvothermal method with the surfactant of PVP. The product showed a stable discharge capacity of 110 mAh g^{-1} after 70 cycles at 1/30 C rate. Goodenough et al. [23] adopted a solvothermal method with ethylenediamine as a surfactant to synthesize hierarchical $LiFePO_4$ porous microspheres assembled with nanoplates, which achieved a discharge capacity of 86 mAh g^{-1} at 10 C rate.

Herein, we propose an alternative approach to the synthesis of hierarchical $LiFePO_4$ microflowers self-assembled by a number of stacked rectangular nanoplates via a solvothermal reaction in ethanol solvent by using self-prepared ammonium iron phosphate rectangular nanoplates as a precursor, which is obtained by a simple water evaporation method. When the ethanol solvent is replaced with the water–ethanol mixed solvent in the solvothermal reaction, only $LiFePO_4$ micro-octahedrons can be prepared. Both of them are carbon-coated through post-heat treatment, respectively. When used as cathode materials in lithium-ion batteries, the hierarchical micro/nanostructured $LiFePO_4$ microflowers show enhanced electrochemical performances compared with $LiFePO_4$ micro-octahedrons, which demonstrates an effective way to improve the electrochemical properties of $LiFePO_4$ nanomaterials.

2. Experimental

All chemicals were purchased from China and used as raw materials without further purification.

2.1. Synthesis of the precursor via a water evaporation method

The synthesis of the precursor was a simple water evaporation method, which was introduced in our previous paper [24]. 3.45 g of $NH_4H_2PO_4$ and 2.7 g of $FeCl_3$ were dissolved in 40 mL of distilled water in a beaker with stirring. Then the beaker was kept in a fan-forced oven at 140 °C for 4 h. As time passed, water, as the solvent in the solution, was gradually evaporated. Finally a dry white powder was deposited on the bottom of the beaker. The powder was collected and washed with distilled water and ethanol for several times, and dried in air at 60 °C for 2 h.

2.2. Synthesis of $LiFePO_4$ via a solvothermal method

0.221 g of the as-prepared precursor, 0.213 g of LiCl and 0.15 mL of $N_2H_4{\cdot}H_2O$ aqueous solution (10 M) were added in 40 mL of ethanol with vigorous stirring. Then the mixture was sealed in 50 mL stainless-steel autoclave and heated in an oven at 170 °C for 24 h. After cooling to ambient temperature, a light green precipitate was obtained and washed with H_3PO_4 aqueous solution (pH 2–3) and distilled water for several times, and then dried in vacuum at 100 °C for 1 h.

2.3. Modification of $LiFePO_4$ with carbon-coating

0.1 g of glucose and 1.9 g of the as-synthesized $LiFePO_4$ were dispersed in 5 mL of distilled water by ultrasonication to form thick slurry and then stirred for 1 h till a fine mixture was formed, and dried at 60 °C for 2 h. The samples were first heated at 350 °C for 4 h and then at 650 °C for 9 h in a tube furnace with N_2 atmosphere in order to carbonize the glucose and increase the crystallinity of the $LiFePO_4$ samples.

2.4. Characterization

X-ray powder diffraction (XRD) patterns were recorded on a Japan Rigaku D/max-rB X-ray diffractometer with Cu Kα radiation

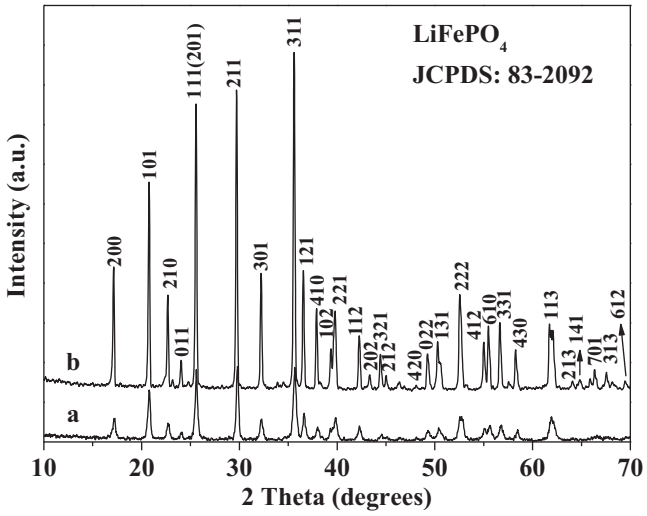

Fig. 1. XRD patterns of the samples prepared in ethanol solvent by solvothermal reaction (a) and then modified with carbon-coating (b).

(λ = 0.15418 nm), operated at 40 kV and 80 mA. Field-emission scanning electron microscopy (FESEM) measurement was carried out with a FEI Siron 200 field-emission scanning electron microscope, operated at an acceleration voltage of 10 kV. Transmission electron microscopic (TEM) images and high resolution TEM images (HRTEM) were taken with a Philips CM 20 FEG and JEOL-2010 transmission electron microscope respectively, operated at an accelerating voltage of 200 kV.

2.5. Electrochemical characterization

The electrochemical properties of the as-prepared samples were characterized by coin-type cells (CR2032) with lithium foil as counter electrode. A composite electrode was prepared by mixing the $LiFePO_4$, carbon black, and polyvinylidene fluoride (PVDF) in weight ratio of 80:15:5 in *n*-methyl pyrrolidinone (NMP) solvent. The obtained slurry was then cast onto aluminum foil with the slurry thickness controlled. After the evaporation of the solvent by a mild heating, the cathode was roll-pressed and further dried in vacuum at 120 °C for 5 h. The thickness of the cast electrode materials is about 28 μm. Finally, coin-type cells (CR2032) were assembled in an Ar-filled dry glove box. The liquid electrolyte used was 1 M $LiPF_6$ in a 1:1 mixture of ethylene carbonate (EC) and dimethyl carbonate (DMC), and the separator was Celgard 2400 micro-porous polypropylene membrane.

Galvanostatical charge and discharge was controlled between 2.5 and 4.2 V on a multi-channel battery tester (Neware Battery Testing System, Shenzhen Neware Electronic Co., China) at room temperature. The cyclic voltammetry tests (CV) were carried out on a CHI604C electrochemical workstation (Shanghai Chenhua Instrument Co., China) at a scanning rate of 0.05 mV s^{-1} from 2.5 to 4.2 V (versus Li^+/Li) at room temperature.

3. Results and discussion

The composition and phase purity of the products were examined by X-ray diffraction. Fig. 1a shows the XRD pattern of the sample prepared in ethanol solvent by solvothermal reaction. All diffraction peaks agree well with those of phospho-olivine $LiFePO_4$ indexed with orthorhombic *Pnma* space group (JCPDS No. 83-2092). To be noted that without H_3PO_4 aqueous solution washing, the product often contains Li_3PO_4 as impurity (Fig. S1). Fig. 1b shows the XRD pattern of the carbon-coated sample $LiFePO_4$ which

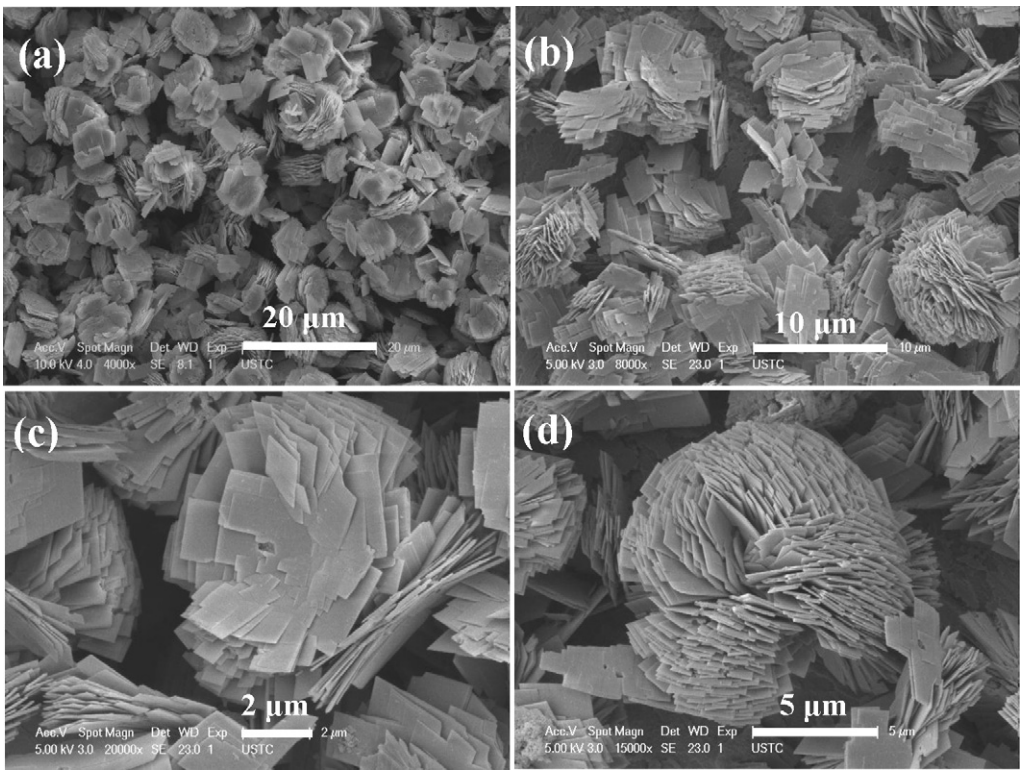

Fig. 2. FESEM images of the $LiFePO_4$ sample modified with carbon-coating. (a) Low magnification, (b) high magnification, (c) a hierarchical microflower with ends of the rectangular nanoplates merged together, and (d) a hierarchical microflower with full of rectangular nanoplates as petals.

is obtained at 600 °C in N_2 atmosphere for 5 h. The diffraction peaks of the sample become much sharper, suggesting improved crystallinity of $LiFePO_4$. On the other hand, there is no additional diffraction peaks associated with crystal modification by carbon, which indicates that the carbon generated from glucose is amorphous and its presence does not influence the structure of $LiFePO_4$.

The field-emission scanning electron microscopy is used to observe the morphologies of the as-prepared products. Fig. 2 shows the FESEM images of the carbon-coated $LiFePO_4$ sample. It is mainly composed of hierarchical microflowers with diameters of about 6–8 μm (Fig. 2a). Higher magnification FESEM image in Fig. 2b indicates that the $LiFePO_4$ hierarchical microflower is assembly of rectangular nanoplates with length of 6–8 μm, width of 1–2 μm and thickness of around 50 nm. Fig. 2c shows that the ends of the nanoplates have been merged together and constructed the middle part of the flower. Fig. 2d reveals that the microflower can be assembled like a microsphere with plenty of rectangular nanoplates as petals.

Further insight into the morphology and microstructure of the $LiFePO_4$ hierarchical microflowers has been gained with the help of TEM and HRTEM. Fig. 3a shows a TEM image of single hierarchical microflower prepared in ethanol solvent by solvothermal reaction. From its edges, one can see that it is composed of many nanoplates with rectangular angles. Fig. 3b presents the morphology of a single rectangular nanoplate. The inserted SAED pattern viewed along zone axis of [1 0 0] implies its single crystalline nature. HRTEM image in Fig. 3c shows the clear crystal lattices of the nanoplate in Fig. 3b. The lattice interplanar spacings of 0.23 nm and 0.29 nm are corresponding to the (0 0 2) and (0 2 0) planes of orthorhombic $LiFePO_4$, respectively.

In order to understand how the precursor can be transformed into hierarchical $LiFePO_4$ microflowers, Fig. S2 shows the structure and morphology of the precursor prepared by a simple water evaporation method. The XRD pattern (Fig. S2a) could be indexed to $NH_4FeP_2O_7{\cdot}1.5H_2O$ (JCPDS 31-0054). The low magnification FESEM image (Fig. S2b) indicates that the precursor is composed of nanoplates in large scale. The high magnification FESEM image (Fig. S2c) reveals that each nanoplate almost has rectangular shape with length of 3–4 μm, width of about 1 μm and thickness of about 150 nm, which is further confirmed by the TEM images in Fig. S2d and e.

During the solvothermal reaction, the $NH_4FeP_2O_7{\cdot}1.5H_2O$ nanoplate precursor can be reduced by N_2H_4 and intercalated by Li^+ ions in ethanol to form $LiFePO_4$ nanoplates. Due to high surface energy, these thin nanoplates are not stable in ethanol solvent under solvothermal conditions. They tend to grow into microflowers which are assembled with multilayered nanoplates, as shown in Fig. S3. It can be seen that the carbon-modified $LiFePO_4$ retains the original morphology from the $LiFePO_4$ sample prepared by the solvothermal process. These nanoplates have slightly larger sizes in width and length and thinner thickness compared with the $NH_4FeP_2O_7{\cdot}1.5H_2O$ nanoplate precursor. We speculate that the formation of these nanoplates is probably an *in situ* conversion from the precursor coupled with Ostwald ripening, which is similar to the formation process of Ba_2WO_6 hierarchical microspheres from interconnected square nanoplates by using PVP as the surfactant [25].

When ethanol is replaced with the water–ethanol mixed solvent in the solvothermal reaction and the other reaction conditions are the same, $LiFePO_4$ micro-octahedrons instead of hierarchical microflowers can be prepared. Fig. S4 shows the XRD pattern and FESEM images of $LiFePO_4$ micro-octahedrons prepared in water–ethanol mixed solvent ($V_{H_2O} : V_{C_2H_5OH} = 1 : 7$). The $LiFePO_4$ micro-octahedrons have length of 3–4 μm and thickness of 2 μm. The results indicate that the $NH_4FeP_2O_7{\cdot}1.5H_2O$ precursor could be dissolved in water under the solvothermal condition, and the $LiFePO_4$ microcrystals would grow from the mixed solvent

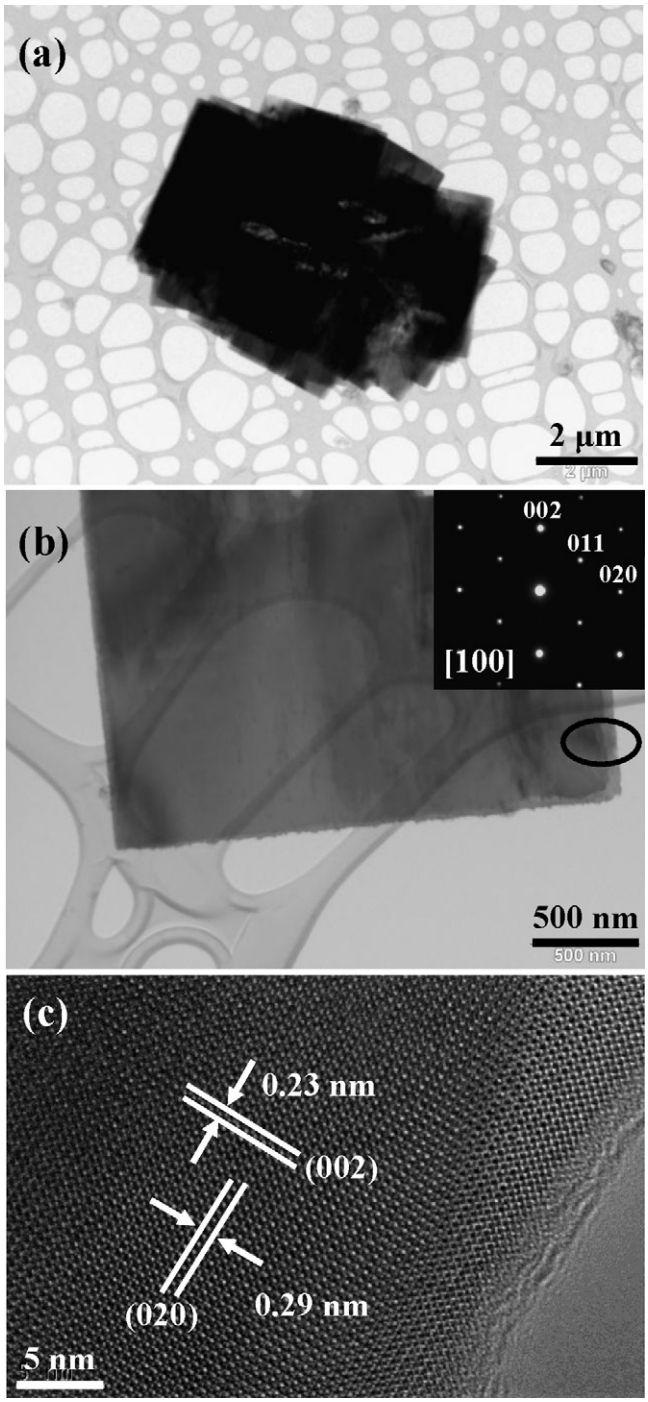

Fig. 3. TEM and HRTEM images of the $LiFePO_4$ microflower prepared in ethanol solvent by solvothermal reaction. (a) A hierarchical microflower, (b) high-magnification TEM image of an individual nanoplate (inset: SAED pattern), and (c) HRTEM image of the nanoplate shown in (b).

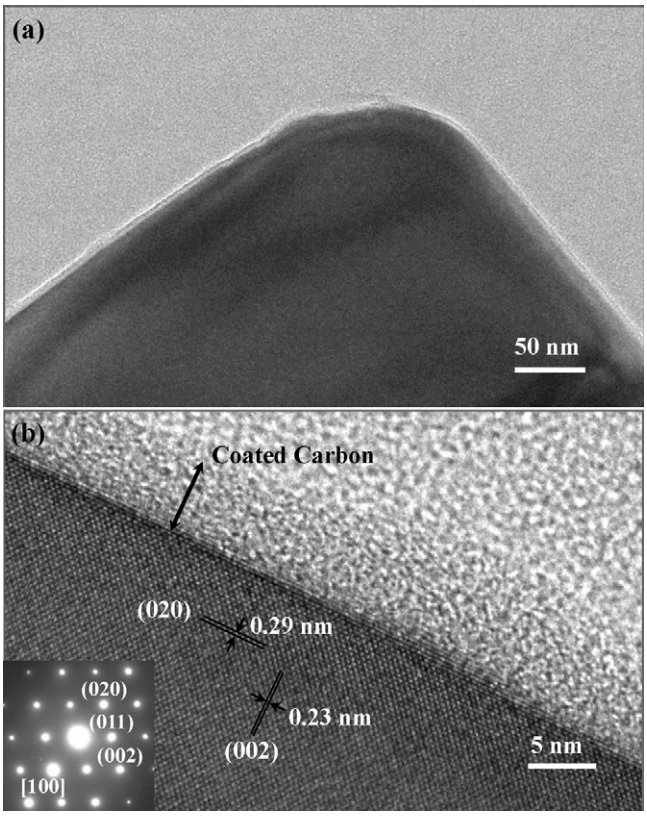

Fig. 4. TEM and HRTEM images of an individual nanoplate of the $LiFePO_4$ microflower modified with carbon-coating. (a) High-magnification TEM image and (b) HRTEM image. Inset: SAED pattern of the nanoplate shown in (b).

spontaneously into the octahedron shapes without the precursor's templating.

TEM and HRTEM have also been used to observe the morphology and microstructure of the carbon coated $LiFePO_4$ hierarchical microflowers (Fig. 4) and micro-octahedrons (Fig. S5), respectively. Fig. 4a shows the high magnification TEM image of part of a single rectangular nanoplate of the carbon-coated $LiFePO_4$ microflower. It can be seen that the edge of the nanoplate is coated with an even-distributed amorphous layer. The high resolution HRTEM image in Fig. 4b clearly displays that the thickness of the layer is about 5 nm. The inserted SAED pattern viewed along zone axis of [1 0 0] still implies its single crystalline nature, indicating that the crystal structure of $LiFePO_4$ has not been changed due to the modification with carbon-coating. It can also be observed that the lattice interplanar spacings of 0.23 nm and 0.29 nm are corresponding to the (0 0 2) and (0 2 0) planes of orthorhombic $LiFePO_4$, respectively. But the coated-carbon layer is amorphous, without any obvious lattice fringes. Fig. S5a presents the TEM image of part of a carbon-coated $LiFePO_4$ micro-octahedron. It can also be seen that there exists an amorphous carbon layer coated on the surface of the $LiFePO_4$ micro-octahedron with a thickness about 5 nm in the high magnification TEM image (Fig. S5b). The coated carbon content of modified hierarchical $LiFePO_4$ microflowers and $LiFePO_4$ micro-octahedrons was measured with a Carbon Sulfur Automatic Analyzer (HH2000A, Wuxi Chuangxiang Co. China). The results indicate that the coated carbon contents of modified hierarchical $LiFePO_4$ microflowers and $LiFePO_4$ micro-octahedrons are 1.21 and 1.23 wt.%, respectively. Both of them have similar carbon content.

The electrochemical performances of the two modified $LiFePO_4$ samples with different morphologies have been investigated. The $LiFePO_4$ micro-octahedrons were also modified with carbon-coating under the same conditions for $LiFePO_4$ microflowers. The initial charge–discharge profiles are obtained from coin-type cells, at a current density varying from 0.1 C (15 mA g^{-1}) to 10 C (1500 mA g^{-1}) rate between 2.5 and 4.2 V, as shown in Fig. 5a and b, respectively. To be noted that the charge/discharge capacities was based on the total weight of bare $LiFePO_4$ and the coated-carbon. The cells were charged at the same rate of 0.5 C to insure identical conditions for each discharge. Fig. 5a shows that the hierarchical $LiFePO_4$ microflower sample with carbon-coating delivers an initial discharge capacity of 162 mAh g^{-1} at 0.1 C. The voltage profile drops rapidly from the end-charging voltage (4.2 V)

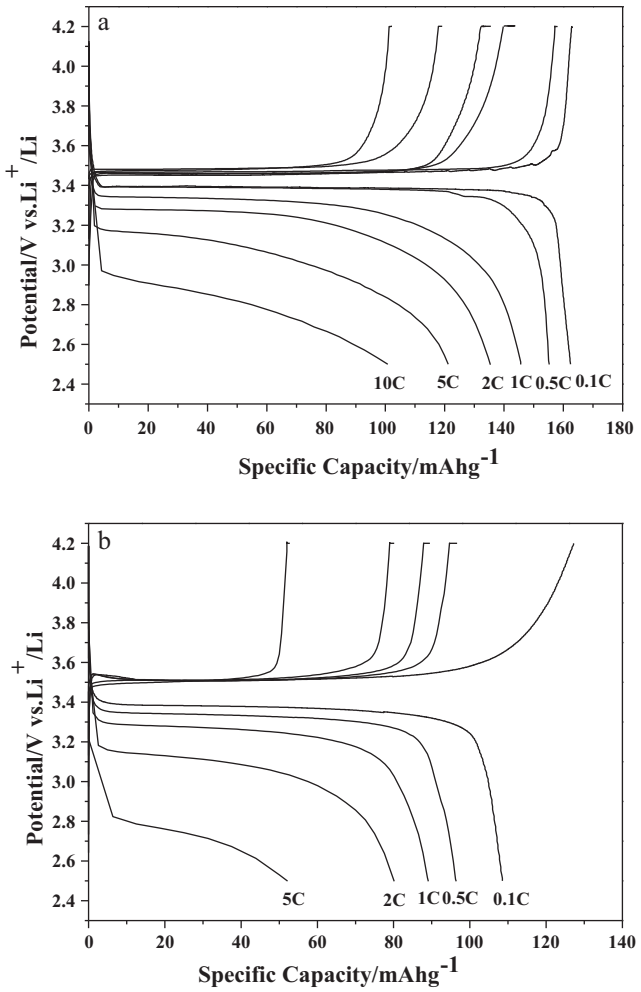

Fig. 5. Charge–discharge profiles of carbon-coated $LiFePO_4$ samples at different discharge rates. (a) Hierarchical microflowers and (b) micro-octahedrons.

to about 3.4 V. Then this voltage is kept almost constant during the following intercalation and more than 80% of the discharge occurs at a flat voltage plateau near 3.39 V. Whereas the $LiFePO_4$ micro-octahedrons with carbon-coating only delivers an initial discharge capacity of 108 mAh g^{-1} at 0.1 C shown in Fig. 5b. 59% of the discharge occurs at a voltage plateau near 3.37 V. Moreover, the plateau voltage difference could reflect the polarization effect during the electrochemical reaction [26]. For the modified hierarchical microflower sample about 70 mV plateau voltage difference is observed between charge and discharge at 0.1 C rate, but for the modified micro-octahedron sample the plateau voltage difference is as high as 140 mV at 0.1 C rate. It clearly demonstrates that the polarization of the modified hierarchical microflower sample is much less than the modified micro-octahedron sample.

Fig. 6 further compares the rate capability and cycle performance of the two carbon-coated $LiFePO_4$ samples. The initial discharge capacity of the hierarchical $LiFePO_4$ microflower sample with carbon-coating presents a high value of 154 mAh g^{-1} at 0.5 C (Fig. 5a). Fig. 6a shows that when the discharge rate is increased to 1, 2, 5 and 10 C, the modified microflower sample delivers initial discharge capacity of 146, 135, 121 and 101 mAh g^{-1}, respectively. While the $LiFePO_4$ micro-octahedron sample with carbon-coating only presents initial discharge capacity of 96 mAh g^{-1} at 0.5 C (Fig. 5b). Fig. 6b shows that when the discharge rate is increased to 1, 2 and 5 C rates, the modified micro-octahedron sample only presents initial discharge capacity of 89, 80 and 52 mAh g^{-1},

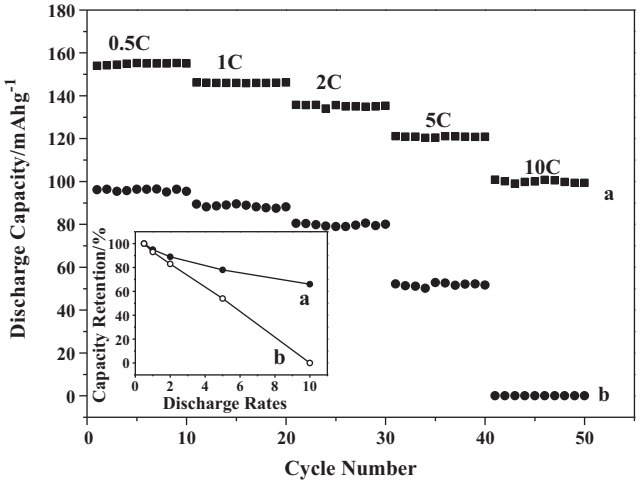

Fig. 6. Comparison of the rate capabilities of carbon-coated $LiFePO_4$ samples. (a) Hierarchical microflowers and (b) micro-octahedrons. Inset: their capability retention at different rates.

respectively and when the discharge rate is increased to 10 C, it hardly presents discharge capacity because of the huge polarization during the charge–discharge process. Fig. 6 also reveals the 10-cycle performances of the two carbon-coated samples. It can be seen that both of them have good discharge capacity stability at these different rates. However, they exhibit quite different capacity decay with the increased rate. As shown in the inset of Fig. 6, the modified hierarchical $LiFePO_4$ microflower sample shows much slower capacity decay than the modified micro-octahedron sample, especially at high rates.

Furthermore, Fig. 7 shows the cycling performance of the hierarchical $LiFePO_4$ microflower sample with carbon-coating to extended cycles. The sample delivers a high discharge capacity of 146 mAh g^{-1} in the first cycle, and could remain 143 mAh g^{-1} after 70 cycles at 1 C rate, indicating that this modified hierarchical microflower sample has good cycling stability. The cycling performance of the modified hierarchical $LiFePO_4$ is better than some reported $LiFePO_4$ nanoparticles [27,28]. Although most of the literatures claimed that the $LiFePO_4$ had good cycling performance [4,5,9,10], but recently some groups reported that the $LiFePO_4$ nanoparticles had an obvious capacity fading during cycling process [19,27–30]. This capacity degradation is mainly because the

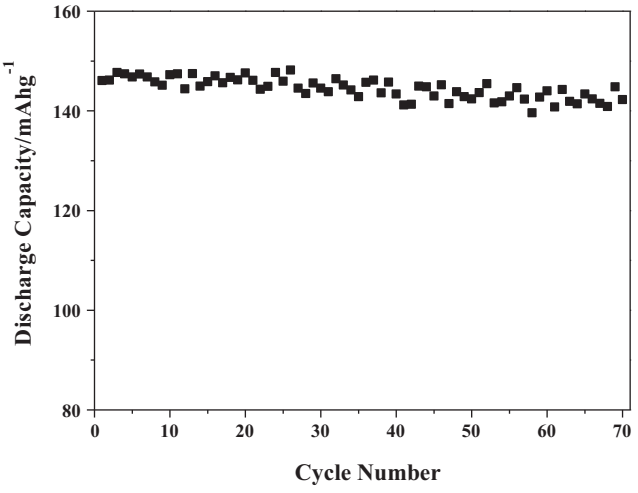

Fig. 7. Cycling performance of the carbon-coated $LiFePO_4$ microflower sample at 1 C rate between 2.5 and 4.2 V.

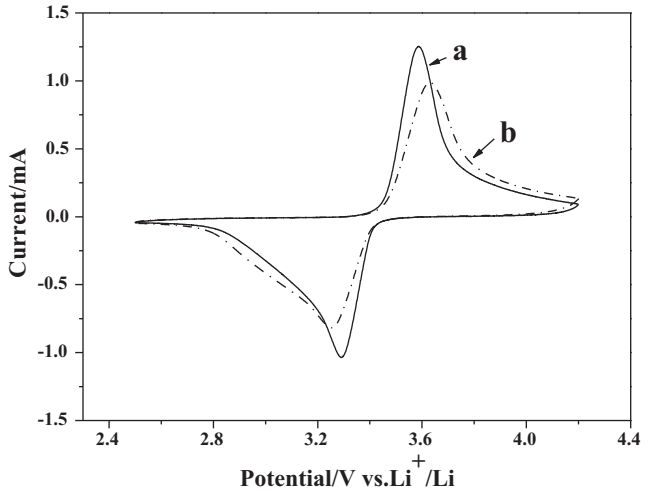

Fig. 8. Cyclic voltammograms of carbon-coated $LiFePO_4$ samples. (a) Hierarchical microflowers and (b) micro-octahedrons. The scanning rate is 0.05 mV s^{-1} between 2.5 and 4.2 V.

nanosized $LiFePO_4$ would be etched by residual HF in $LiPF_6$/DMC + EC electrolyte, which leads to the loss of active materials and separation of active materials from conductive carbon. These $LiFePO_4$ microflowers have relatively smaller contact areas with electrolyte and better structure stability compared with $LiFePO_4$ nanoplates as the building blocks, which results in its enhanced cycling performance. The tap density of the carbon-coated $LiFePO_4$ microflower is 1.17 g cm^{-3}, which is bigger than normal nanomaterials. This can be attributed to the micro-size of its assemblies [23].

The influence of morphology on the electrochemical properties of carbon-coated $LiFePO_4$ is further investigated by cyclic voltammetry. The carbon-coated hierarchical $LiFePO_4$ microflower and the micro-octahedron samples are tested at a scanning rate of 0.05 mV s^{-1} between the voltage limit of 2.5 and 4.2 V (Li/Li^+) and the cyclic voltammograms (CV) profiles of them are shown in Fig. 8, respectively. The carbon-coated microflower sample exhibits an anodic peak at 3.29 V and a corresponding cathodic response at 3.57 V and the potential interval of it is 0.28 V, whereas the carbon-coated micro-octahedron sample exhibits an anodic peak at 3.24 V and a corresponding cathodic response at 3.64 V and the potential interval of it is 0.40 V. The hysteresis is similar to that observed in galvanostatic cycling of carbon-coated $LiFePO_4$ microflowers and micro-octahedrons in Fig. 5. The more symmetric and spiculate peak profile for carbon-coated $LiFePO_4$ microflowers indicates a reversible elctrochemical reaction during lithium ion insertion and extraction [31]. Compared with $LiFePO_4$ micro-octahedrons, the thin nanoplates as the building blocks assembled in $LiFePO_4$ microflowers can shorten the lithium ion diffusion path greatly, which can enhance the electrochemical reaction kinetics, reduce the polarization and improve its rate performance.

4. Conclusions

In this paper, we have successfully prepared hierarchical $LiFePO_4$ microflowers via a solvothermal reaction in ethanol solvent by using the self-prepared ammonium iron phosphate rectangular nanoplates as a precursor, which is obtained by a simple water evaporation method beforehand. The hierarchical $LiFePO_4$ microflowers with diameters of 6–8 μm are self-assemblies of a number of stacked rectangular nanoplates with length of 6–8 μm, width of 1–2 μm and thickness of around 50 nm under solvothermal condition and without any surfactant. When the water–ethanol mixed solvent is used instead of the ethanol solvent, $LiFePO_4$ micro-octahedrons with lengths of 3–4 μm and thickness of 2 μm can be prepared. Then they are respectively modified with carbon coating through a post-heat treatment and their morphologies are retained. As a cathode material for rechargeable lithium ion batteries, the carbon-coated hierarchical $LiFePO_4$ microflowers show enhanced electrochemical performances compared with carbon-coated $LiFePO_4$ micro-octahedrons. They deliver an initial discharge capacity of 162 mAh g^{-1} at 0.1 C rate and a discharge capacity of 101 mAh g^{-1} even at the discharge rate up to 10 C. In addition, they exhibit good cycle performance, and it only decreases 3 mAh g^{-1} after 70 charge–discharge cycles at a rate of 1 C. Such hierarchical micro/nanostructures take the advantages of both nanometer-sized building blocks and micro-sized assemblies. It facilitates fast electrochemical reaction kinetics and good electrochemical stability. This novel hierarchical microflower $LiFePO_4$ material with carbon coating is anticipated to satisfy the industrial needs in electric vehicles (EV), hybrid electric vehicles (HEV), and other mobile or portable electric devices.

Acknowledgments

This work has been supported by the National Natural Science Foundation of China (NSFC Grants 20871038, 21176054 and 20976033), the Fundamental Research Funds for the Central Universities (2010HGZY0012) and the Education Department of Anhui Provincial Government (TD200702). We thank Mr. J. Xu in City University of Hong Kong for a useful discussion in crystal structure.

Appendix A. Supplementary data

Supplementary data associated with this article can be found, in the online version, at doi:10.1016/j.jpowsour.2011.08.046.

References

[1] J.M. Tarascon, M. Armand, Nature 414 (2001) 359–367.
[2] M.S. Whittingham, Chem. Rev. 104 (2004) 4271–4301.
[3] K. Zaghib, P. Charest, A. Guerfi, J. Shim, M. Perrier, K. Striebel, J. Power Sources 134 (2004) 124–129.
[4] A.K. Padhi, K.S. Nanjundasawamy, J.B. Goodenough, J. Electrochem. Soc. 144 (1997) 1188–1194.
[5] A.K. Padhi, K.S. Nanjundaswamy, C. Masquelier, S. Okada, J.B. Goodenough, J. Electrochem. Soc. 144 (1997) 1609–1613.
[6] S.Y. Chung, J.T. Bloking, Y.M. Chiang, Nat. Mater. 1 (2002) 123–128.
[7] N. Meethong, Y.H. Kao, S.A. Speakman, Y.M. Chiang, Adv. Funct. Mater. 19 (2009) 1060–1070.
[8] H.P. Subramanya, B. Ellis, N. Coombs, L.F. Nazar, Nat. Mater. 3 (2004) 147–152.
[9] H.M. Xie, R.S. Wang, J.R. Ying, L.Y. Zhang, A.F. Jalbout, H.Y. Yu, G.L. Yang, X.M. Pan, Z.M. Su, Adv. Mater. 18 (2006) 2609–2613.
[10] H. Huang, S.C. Yin, L.F. Nazar, Electrochem. Solid-State Lett. 4 (2001) A170–A172.
[11] P.G. Bruce, B. Scrosati, J.M. Tarascon, Angew. Chem. Int. Ed. 47 (2008) 2930–2946.
[12] T. Muraliganth, A.V. Murugan, A. Manthiram, J. Mater. Chem. 18 (2008) 5661–5668.
[13] A.V. Murugan, T. Muraliganth, A. Manthiram, J. Phys. Chem. C 112 (2008) 14665–14671.
[14] E. Hosono, Y.G. Wang, H.S. Zhou, ACS Appl. Mater. Interfaces 2 (2010) 212–218.
[15] S.Y. Lim, C.S. Yoon, J.P. Cho, Chem. Mater. 20 (2008) 4560–4564.
[16] K. Saravanan, P. Balaya, M.V. Reddy, H. Gong, B.V.R. Chowdari, J.J. Vittal, Energy Environ. Sci. 3 (2010) 457–464.
[17] R. Amin, P. Balaya, J. Maier, Electrochem. Solid-State Lett. 10 (2007) A13–A16.
[18] Y.G. Wang, Y.R. Wang, E. Hosono, K.X. Wang, H.S. Zhou, Angew. Chem. Int. Ed. 47 (2008) 7461–7465.
[19] X.K. Zhi, G.C. Liang, L. Wang, X.Q. Ou, J.P. Zhang, J.Y. Cui, J. Power Sources 189 (2009) 779–782.
[20] Y.G. Guo, J.S. Hu, L.J. Wan, Adv. Mater. 20 (2008) 2878–2887.
[21] X.L. Wu, L.Y. Jiang, F.F. Cao, Y.G. Guo, L.J. Wan, Adv. Mater. 21 (2009) 2710–2714.
[22] H. Yang, X.L. Wu, M.H. Cao, Y.G. Guo, J. Phys. Chem. C 113 (2009) 3345–3351.
[23] C.W. Sun, S. Rajasekhara, J.B. Goodenough, F. Zhou, J. Am. Chem. Soc. 133 (2011) 2132–2135.
[24] J. Xu, W.X. Zhang, Z.H. Yang, S.X. Ding, C.Y. Zeng, L.L. Chen, Q. Wang, S.H. Yang, Adv. Funct. Mater. 19 (2009) 1759–1766.
[25] Y.Y. Li, J.P. Liu, X.T. Huang, G.Y. Li, Cryst. Growth Des. 7 (2007) 1350–1355.

[26] K. Saravanan, M.V. Reddy, P. Balaya, H. Gong, B.V.R. Chowdari, J.J. Vittal, J. Mater. Chem. 19 (2009) 605–610.
[27] S.B. Lee, S.H. Cho, J.B. Heo, V. Aravindana, H.S. Kim, Y.S. Lee, J. Alloys Compd. 488 (2009) 380–385.
[28] K. Kim, J.H. Jeong, I.J. Kim, H.S. Kim, J. Power Sources 167 (2007) 524–528.
[29] K. Striebel, J. Shim, A. Sierra, H. Yang, X.Y. Song, R. Kostecki, K. McCarthy, J. Power Sources 146 (2005) 33–38.
[30] H.F. Jin, Z. Liu, Y.M. Teng, J.K. Gao, Y. Zhao, J. Power Sources 189 (2009) 445–448.
[31] H.C. Shin, W.I. Cho, H. Jang, J. Power Sources 159 (2006) 1383–1388.